Impact of near-inertial waves on vertical mixing and air-sea CO_2 fluxes in the Southern Ocean

Hajoon Song[1], John Marshall [2], Jean-Michel Campin [2]and Dennis J. McGillicuddy Jr. [3]

[1]Department of Atmospheric Sciences, Yonsei University, Seoul, Republic of Korea
[2]Department of Earth, Atmospheric and Planetary Sciences, Massachusetts Institute of Technology, Cambridge, Massachusetts, USA
[3]Department of Applied Ocean Physics and Engineering, Woods Hole Oceanographic Institution, Woods Hole, Massachusetts, USA

Key Points:

- Filtering out near-inertial waves from a simulation diminishes vertical shear, shallowing the mixed layer depth.
- The shallowed mixed-layer reduces the supply of dissolved inorganic carbon to the surface.
- These high frequency processes can change CO_2 flux by 1/3 amplitude of the seasonal cycle.

Corresponding author: H. Song, hajsong@yonsei.ac.kr

Abstract

We report the significant impact of near-inertial waves (NIWs) on vertical mixing and air-sea carbon dioxide (CO_2) fluxes in the Southern Ocean (SO) using a biogeochemical model coupled to an eddy-rich ocean circulation model. The effects of high-frequency processes are quantified by comparing the fully coupled solution (ONLINE) to two offline simulations based on five-day averaged output of the ONLINE simulation: one that uses vertical mixing archived from the ONLINE model (CTRL) and another in which vertical mixing is recomputed from the five-day average hydrodynamic fields (5dAVG). In this latter simulation, processes with temporal variabilities of a few days including NIWs are excluded in the biogeochemical simulation. Suppression of these processes reduces vertical shear and vertical mixing in the upper ocean, leading to decreased supply of carbon-rich water from below, less CO_2 outgassing in austral winter, and more uptake in summer. The net change amounts up to 1/3 of the seasonal variability in SO CO_2 flux. Our results clearly demonstrate the importance of resolving high frequency processes such as NIWs to better estimate the carbon cycle in numerical model simulations.

1 Introduction

Intensive vertical mixing is one of the important aspects that characterize the Southern Ocean (SO) [*de Boyer Montégut et al.*, 2004; *Holte et al.*, 2017]. To the north of the Antarctic Circumpolar Current (ACC), thick mixed layers in austral winter reach a few hundred meters deep and contribute to the exchanges of momentum, heat and freshwater, and formation of Antarctic Intermediate Water and Subantarctic Mode Water [*Dong et al.*, 2008]. Deep vertical mixing is also important in biogeochemical processes. It brings surface water, rich in oxygen, to the interior ocean during the process of intermediate and mode water formations and forms the oxygen maximum layer [*Talley et al.*, 2011]. The uptake of anthropogenic tracers (e.g. chlorofluorocarbons) can be expedited through deep convection [*Shao et al.*, 2013; *Song et al.*, 2015]. Intensive vertical mixing is also efficient in drawing the subsurface water mass rich in nutrients and carbon close to the surface. For example, iron, critical for the primary production in the SO, is supplied from the interior of the ocean by vertical mixing in winter [*Tagliabue et al.*, 2014]. Vertical mixing is claimed to be responsible for the nitrate transport from the deep Eastern South Pacific to the Patagonian shelf region that is one of the most productive areas in the world [*Song et al.*, 2016a].

Near-inertial waves (NIWs) can significantly impact surface vertical mixing. NIWs have a frequency close to an inertial frequency with a length scale of 10 to 100 km and are mainly excited by wind forcing [*Alford et al.*, 2016]. In particular, midlatitude storms can drive the ocean with their inertially rotating components [*D'Asaro*, 1985] and excite high and low mode waves. High modes create counterclockwise rotation in the SO, producing high vertical shear of currents and enhanced vertical mixing with the downward propagation of energy [*Alford et al.*, 2016; *Alford and Gregg*, 2001]. In numerical experiments, NIWs deepen mixed layer depths (MLDs) by up to 30% on annual average between 40°S and 60°S [*Jochum et al.*, 2013]. This deepening of MLDs in the SO is associated with the midlatitude storm tracks [*Simmons and Alford*, 2012], which is consistent with the view that a high level of wind work can generate NIWs.

The modulation of vertical mixing by NIWs are expected to influence the air-sea CO_2 exchange in the SO. The SO CO_2 flux is controlled by two key processes: biological drawdown and intensive vertical mixing [*Wetzel et al.*, 2005; *Takahashi et al.*, 2009]. In austral summer, the SO takes up CO_2 from the atmosphere with biological processes leading to drawdown, but it emits CO_2 into the atmosphere in austral winter due to the entrainment of carbon-rich interior water up to the surface. It is hence anticipated that enhanced vertical mixing by NIWs promotes more entrainment in austral winter, resulting in more CO_2 outgassing. However, it is not well investigated how much these processes influence air-sea CO_2 exchange. In addition, their role in austral summer is uncertain as biological drawdown is itself impacted by the MLD. Deepening of the MLD in austral summer may enrich the surface ocean with carbon, but at the same time, bring more nutrients that potentially promote higher biological drawdown. If we consider the changes in temperature by mixing that regulates the solubility, it becomes more difficult to anticipate the role of high frequency processes on CO_2 flux.

Here we attempt to quantify the integral effect of NIWs on CO_2 flux near the Drake Passage. Our approach is to compare CO_2 fluxes with and without high temporal variabilities including NIWs by making use of both online and offline biogeochemical models. The online biogeochemical simulation is forced by 6-hourly wind product to properly simulate the input of energy with near inertial frequency. The offline biogeochemical simulation is forced by the same wind forcing, but the ocean states driving biogeochemical variables are the 5-day averaged fields from the online simulation, as described in section 2. The results in section 3 suggest that they are capable of altering the air-sea CO_2 flux significantly through the vertical flux of carbon. Then the discussion on air-sea CO_2 simulation follows in section 4.

2 Simulations of air-sea CO_2 flux

2.1 Eddy-Resolving Model

A simple biogeochemical model [*Dutkiewicz et al.*, 2005; *Parekh et al.*, 2006; *Verdy et al.*, 2007] is coupled to a 1/20° version of the MIT Ocean General Circulation Model (MITgcm) [*Marshall et al.*, 1997a,b; *Adcroft et al.*, 1997; *Marshall et al.*, 1998; *Adcroft et al.*, 2004]. The model domain covers the area from -75°S to -35°S with a 140° longitudinal swath of a section of the Antarctic Circumpolar Current (ACC) stretching from the Southeast Pacific through Drake Passage to the Southwest Atlantic (Fig. 1(a)) and has 50 vertical levels with higher resolution near the surface (10 m). The model configuration is that described in *Tulloch et al.* [2014] and is same as that used in *Song et al.* [2016b]. In particular, the ocean model was integrated with 6-hourly wind and buoyancy fluxes from the reanalysis data set by European Centre for Medium-Range Weather Forecasts [*Simmons et al.*, 2007]. Vertical mixing is parameterized by the nonlocal K-profile parameterization (KPP) scheme of *Large et al.* [1994] in which the depth of the boundary layer is first estimated based on the bulk Richardson number determined by the surface forcing, buoyancy and vertical shear of velocity. Then the vertical diffusivity is calculated within the boundary layer proportionally to its depth. The biogeochemical boundary conditions are provided from the monthly mean states from a global model [*Song et al.*, 2016b]. The integration of this configuration (referred to as ONLINE hereinafter) for 4 years with a time step of 2 minutes results in the ocean states that have similarities to the observed SO states including the high level of mesoscale eddy activities whose spatial scale is $O(100$ km).

In the rotary spectra of velocity shear at 100 m in the model, there are two distinctive lines with elevated power at each latitude: one for the frequency band near zero and the other close to the inertial frequency (Fig. 2a). While the former is associated with geostrophic component, the latter reveals NIWs. Velocity shear rotates counterclockwise with positive frequencies near inertial frequency, f. The rotary spectra of velocity also show enhanced variance near f as well as low frequency (not shown), consistent with that obtained from drifter velocity observations [*Elipot and Lumpkin*, 2008]. The wavenum-

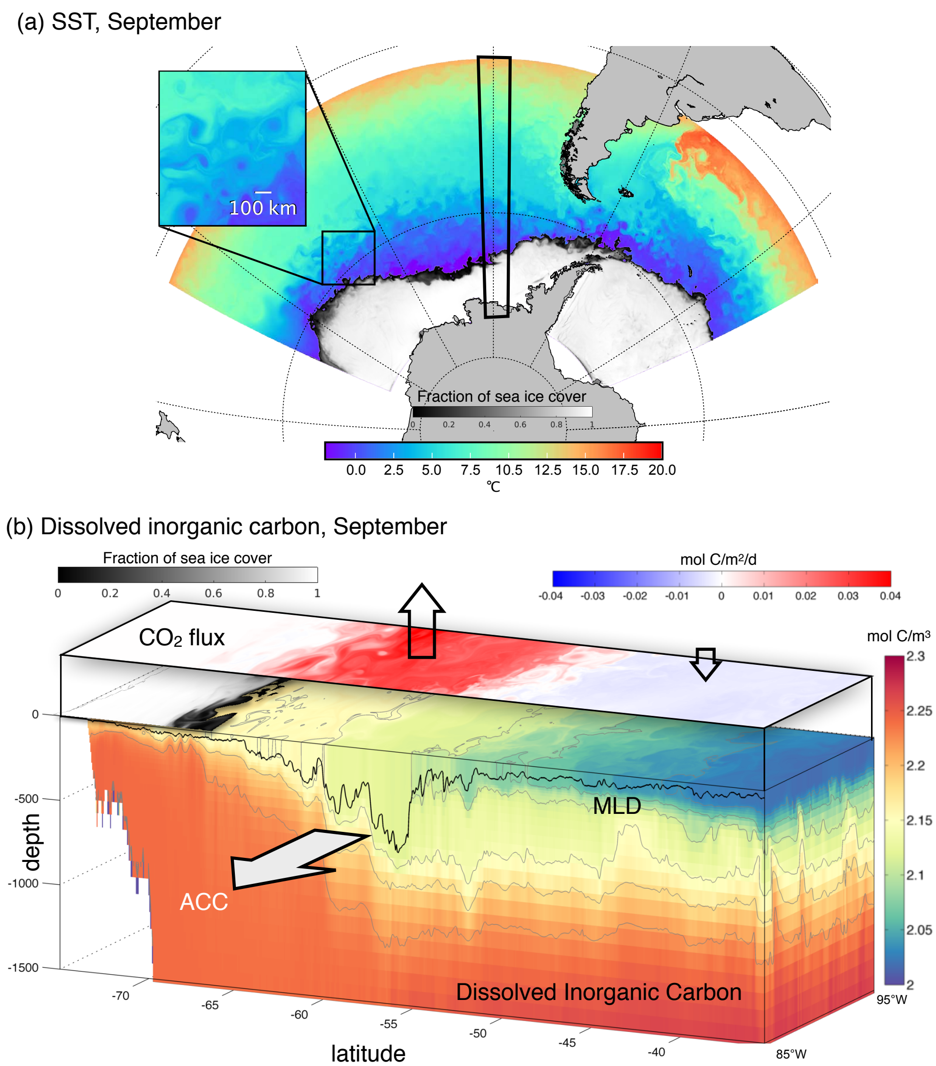

Figure 1. (a) A snapshot of sea surface temperature from the online simulation (ONLINE) in September. The mask in the gray color scale around Antarctica represents the sea ice concentration. The rectangular box at the center indicates the region for the vertical section of dissolved inorganic carbon from the surface to 1500 m in (b). The thin black line in (b) marks the mixed layer depth (MLD) defined as the level whose density is 0.03 kg m^{-3} greater than the surface value. Above the vertical section is the CO_2 flux and the mask in the gray color scale at 0 m is the sea ice concentration. The direction of the ACC is shown as a gray arrow in (b).

ber spectrum using the surface current shows the slope close to k^{-3}, with k being the wavenumber (Fig. 2(c)). Having this slope in the spectrum suggests that mesoscale eddies derive their energy source from baroclinic instability [*Sasaki et al.*, 2014].

2.2 Simulation of air-sea CO_2 flux

The air-sea CO_2 flux (F_{CO_2}) is estimated using a gas exchange parameterization:

$$F_{CO_2} \quad = \quad K_w \, (1 - A_{SI}) \left(p\mathrm{CO_2} - p\mathrm{CO_2}^{atm} \right), \tag{1}$$

where K_w is the gas transfer velocity (m s^{-1}) determined by wind speed squared and sea surface temperature [*Wanninkhof*, 1992], A_{SI} is the fraction of the sea ice coverage within a model grid cell varying from 0 when there is no sea ice to 1 when the grid cell is fully covered by sea ice, and $p\mathrm{CO_2}$ and $p\mathrm{CO_2}^{atm}$ are the oceanic and atmospheric partial pressure of CO_2, respectively. We fix $p\mathrm{CO_2}^{atm}$ at the pre-industrial level (278 ppm) and oceanic surface $p\mathrm{CO_2}$ is estimated using dissolved inorganic carbon (DIC), alkalinity as well as temperature and salinity, following *Follows et al.* [2006].

The distribution of DIC in austral winter reveals the upwelling that increases the surface DIC poleward (Fig. 1(b)). Near Antarctica where the surface DIC is the greatest, the CO_2 outgassing is inhibited by the presence of sea ice. Instead, the strongest CO_2 outgassing occurs near the ACC where the intense vertical mixing increases the surface DIC and, hence, $p\mathrm{CO_2}$. Strong westerly wind forcing also contributes to effective CO_2 outgassing adjacent to the ACC. Interestingly, the sign of CO_2 flux changes near 55°S where the MLD abruptly shallows. The region north of that latitude takes up CO_2 from the atmosphere as $p\mathrm{CO_2}$ becomes smaller than $p\mathrm{CO}_2^{atm}$. Deep mixing can provide iron [*Tagliabue et al.*, 2014] and promote biological drawdown that partially compensates the increase of the surface $p\mathrm{CO_2}$, but its magnitude in our simulation is much less than that of DIC vertical flux because of light limitation in winter. Mesoscale eddies in the model simulations alter DIC concentration as shown in the fluctuating isolines of DIC and hence modulate CO_2 flux by perturbing the concentration of DIC. See *Song et al.* [2016b] for a detailed discussion of the modulation of CO_2 flux by the mesoscale.

2.3 Suppression of NIWs in the biogeochemical model

For the quantification of the impact by NIWs on air-sea CO_2 flux, we designed an offline simulation of the biogeochemical model with suppressed variances in time. This

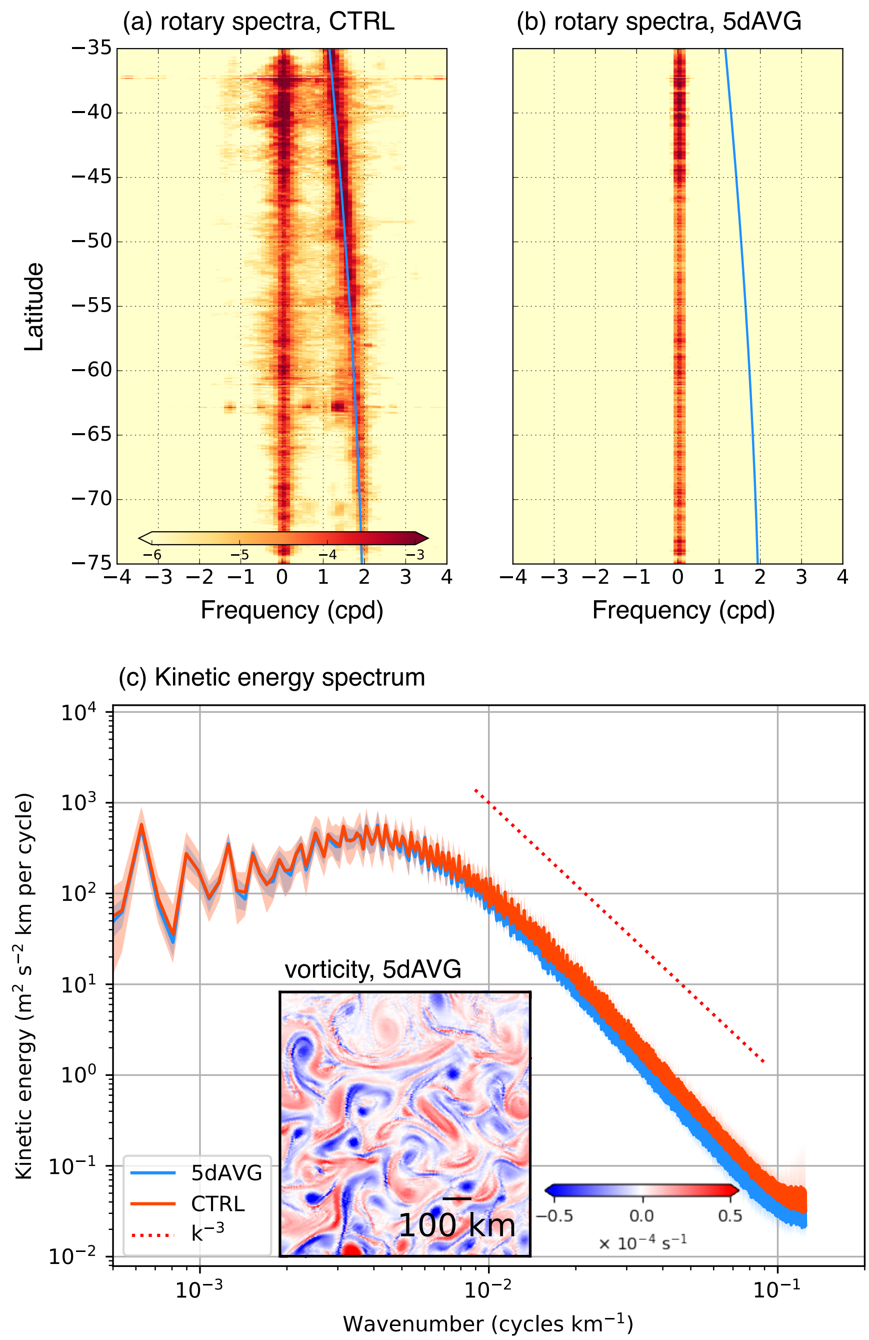

Figure 2. The rotary spectra of vertical shear (s^{-2} cpd^{-1}) in $\log_{10}$ scale at 100 m in the (a)1/20° eddy-resolving model and (b) 5-day averaged velocity. Blue lines in (a, b) represent the inertial frequency, $-f/(2\pi)$, where f is the Coriolis frequency. The kinetic energy spectra of the surface current in ONLINE (red) and 5dAVG (blue) are plotted in (c). Shading indicates the maximum/minimum energy levels during the last 3-year simulation. The inset in (c) is the surface vorticity from 5dAVG.

offline simulation (referred to as 5dAVG hereinafter) was integrated from the second year of ONLINE for 3 years driven by 5-day averaged temperature (T), salinity (S) and horizontal velocities (U, V) from ONLINE. The vertical mixing for tracers was recalculated by the KPP scheme using those 5-day averaged ocean states. The surface forcing is not changed in the surface mixing model and the biogeochemical model.

The 5-day average significantly suppresses the processes with the time scale shorter than a few days, and the peak along f in the variances disappears (Fig. 2(b)). Instead almost all the energy in the vertical shear in 5dAVG is concentrated near zero frequency related to the geostrophic component. The 5-day average slightly lowers the kinetic energy in the wavenumber band corresponding to the mesoscale as well (Fig. 2(c)). However the surface vorticity in 5dAVG shown in the inset of Figure 2(c) shows rich variabilities associated with the mesoscale. Hence, we can interpret the solution from this offline biogeochemical model having a similar phenomenology as ONLINE except the surface vertical mixing with the lack of the energy associated with NIWs.

As the focus of this study lies on the impact of the vertical mixing by NIWs on the CO_2 flux, we designed additional offline biogeochemical simulation where the surface vertical mixing (eddy diffusivity and eddy diffusivity weighted by non-local transport coefficient) from ONLINE were provided to the offline simulation. This offline simulation is referred to as CTRL hereinafter. This CTRL simulation then has the same mean physical oceanic states and surface vertical mixing as ONLINE, and the comparison of CTRL and 5dAVG allows us to isolate the impact of vertical mixing associates with NIWs on CO_2 flux. All three biogeochemical simulations are summarized in Table 1.

3 Impact of NIWs on Mixed Layer Depth and air-sea CO_2 fluxes

3.1 Mixed Layer Depth

The CTRL run captures the observed wintertime MLD structure: deep MLDs reaching deeper than 500 m upstream of Drake Passage (Fig. 1(b)) and relatively shallow MLDs of approximately 150 m in the Atlantic (Fig. 3(a)) [*de Boyer Montégut et al.*, 2004; *Dong et al.*, 2008; *Holte et al.*, 2017]. The absence of NIWs in 5dAVG weakens the vertical mixing and makes the MLD shallower. The reduction in MLD occurs almost everywhere, but it is more pronounced along the ACC where it can be greater than 100 m (Fig. 3(b)).

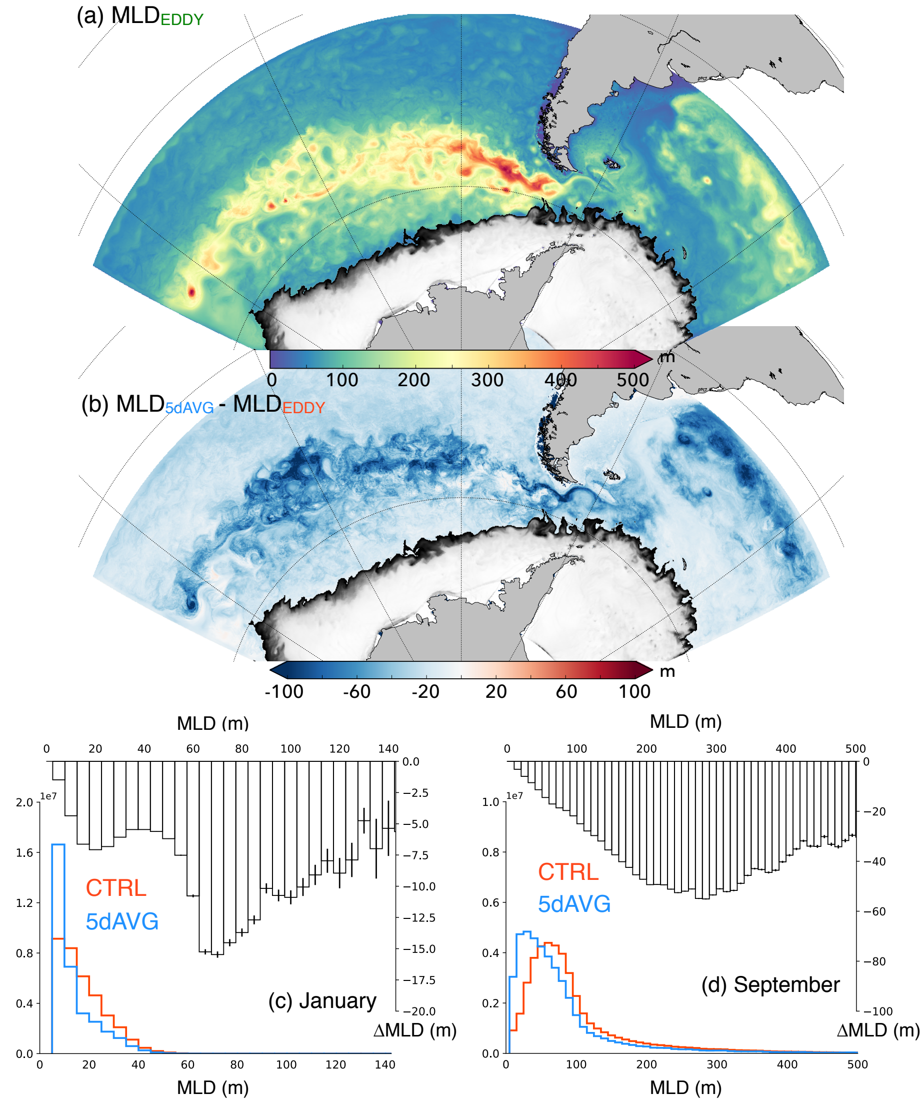

Figure 3. (a) Mixed layer depth (MLD) in the CTRL simulation averaged in September and (b) the changes in MLD between CTRL and 5dAVG. The mask in gray scale is the simulated sea ice fraction. (c) and (d) are histograms of MLDs in CTRL (red) and 5dAVG (blue) in January and September, respectively, with the mean MLD differences (black bar plots) between the two runs binned by the original MLDs in CTRL. Black lines in the bar plots represent the standard errors. Note that the scales in x and y axes are different between (c) and (d).

Table 1. Comparison of biogeochemical simulations. In the table, T, S, u and v represent a snapshot of temperature, salinity, zonal velocity and meridional velocity, respectively, with a frequency of 120 seconds. The 5-day average of those variables are written using angled bracket, $\langle\ \rangle$.

Name	ONLINE	CTRL	5dAVG
Coupling method to the circulation model	online	offline	offline
Physical fields for biogeochemistry	T, S, u, v	$\langle$T$\rangle$, $\langle$S$\rangle$, $\langle$u$\rangle$, $\langle$v$\rangle$	$\langle$T$\rangle$, $\langle$S$\rangle$, $\langle$u$\rangle$, $\langle$v$\rangle$
Eddy diffusivity (κ) in the KPP scheme	computed using T, S, u and v	$\langle\kappa\rangle$ from ONLINE is loaded.	computed using $\langle$T$\rangle$, $\langle$S$\rangle$, $\langle$u$\rangle$ and $\langle$v$\rangle$

The reduction in MLD in 5dAVG can be further evaluated using the histograms of MLDs. In January, the mean MLD in 5dAVG is 12.4 m, approximately 5 m shallower than that in CTRL (Fig. 3(c)). The histogram of 5dAVG is shifted to the left and becomes more skewed: the moment coefficient of skewness is increased from 1.0 to 1.5 when the vertical mixing is recalculated using 5-day averaged fields. The size of MLD reduction increases with the background MLD in CTRL until 70 m, but decreases beyond that point (the black bar plot in Fig. 3(c)). Similar patterns stand out in the MLD changes in September (Fig. 3(d)). The mean MLD in 5dAVG is 83.5 m, which is roughly 24 m shallower than that in CTRL. The histogram of MLD in 5dAVG is more positively skewed than that in CTRL: the moment of coefficient of skewness in 5dAVG is 16.6 while it is 14.7 in CTRL. The reduction of MLD tends to increase as the background MLD becomes deeper, but it starts to decrease with the background MLD for the bins greater than roughly 300 m.

We argue that the reduction of MLD results from the elimination of vertical shear of the current in the near inertial frequency band associated with NIWs (Fig. 2a,b). The depth of surface boundary layer in the KPP mixing scheme is defined as the level where the Richardson number is smaller than a predefined critical value. Since the Richardson number is inversely proportional to the vertical shear of the current, the decrease of vertical shear in 5dAVG can result in the increase of the Richardson number and the reduction of the MLD. Just as the temporal smoothing suppresses the kinetic energy, especially in the mesoscale (Fig. 2(b)), it can alter the stratification near the surface. Suppose, for example, there is a cold eddy that moves along the current in the region of a constant stratification. Taking a 5-day average of the temperature has the effect of the introduction of cold (and heavy) water to the path over the 5-day span and can change the stratification and hence, MLD. However, we find that the 5-day average has little impact on squared Brunt-Väisälä frequency (N^2) in the upper ocean (not shown), suggesting that the MLD reduction is driven mainly by the reduced level of vertical shear with the absence of NIWs in 5dAVG.

3.2 Air-sea CO_2 flux

The CO_2 flux in ONLINE exhibits seasonal variability (red line in Fig. 4(a)). In summer, the ocean takes up CO_2 from the atmosphere while the ocean emits CO_2 back to the atmosphere in winter. This is consistent with previous findings on air-sea CO_2 exchange in the SO [*Lenton et al.*, 2013]. In CTRL where the 5-day averaged fields including vertical mixing drive the biogeochemical model, the ocean takes up more CO_2 in summer and releases more CO_2 in winter (green line in Fig. 4(a)). Although the change in CO_2 flux can be as big as 0.1 Pg C yr^{-1}, the mean difference is rather small (−0.04 Pg C yr^{-1}), suggesting that CTRL is a realistic approximate to ONLINE. When the surface vertical mixing is recalculated using the 5-day averaged fields in 5dAVG, the CO_2 uptake in summer is further enhanced while the outgassing of CO_2 in winter weakens (blue line in Fig. 4(a)). The mean change in CO_2 flux in 5dAVG is −0.23 Pg C yr^{-1} with respect to ONLINE and −0.19 Pg C yr^{-1} with respect to CTRL, with the maximum reduction occurring in winter. The size of the CO_2 flux change in 5dAVG is considerable, with an amplitude of 30% of the seasonal cycle of CO_2 in ONLINE. It is also large when compared with the seasonal cycle of CO_2 in CTRL, roughly 20% of that level.

Suppressing processes with high temporal frequency is responsible for the shift of the CO_2 flux curve of 5dAVG downward compared to that of ONLINE (Fig. 4(a)). Because the surface wind is fixed and the mean temperature is the same, the downward shift of the CO_2 flux curve of 5dAVG is solely the result of the reduction in the surface $p CO_2$. The impact of removing NIWs alone is quantified by comparing CTRL and 5dAVG simulations. Bigger impact is observed in winter and spring, while the summertime shows the

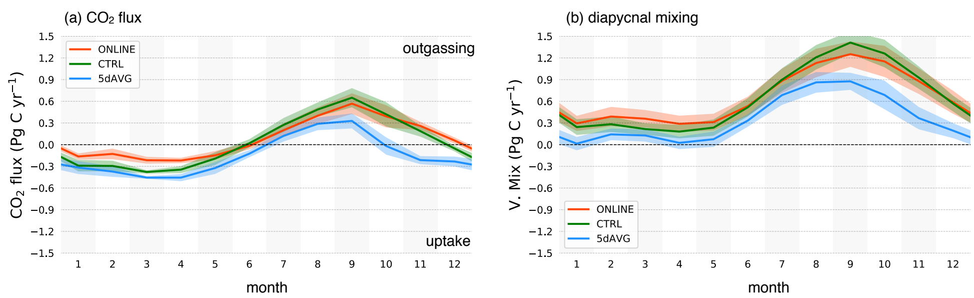

Figure 4. An area integrated (a) CO_2 flux and (b) diapycnal mixing of DIC for each month from ONLINE (red), CTRL (green) and 5dAVG (blue).

minimum impact. This seasonality in the impact of suppressed NIWs is to be expected, given that the main energy source for NIWs is the wind.

To quantitatively investigate the driver of the CO_2 flux changes, we write the DIC concentration thus:

$$\frac{\partial \mathrm{DIC}}{\partial t} = -\nabla \cdot (\mathbf{u}\mathrm{DIC}) + \kappa \frac{\partial^2 \mathrm{DIC}}{\partial z^2} - F_{\mathrm{CO_2}} + S_{\mathrm{bio}} + S_{\mathrm{C}}, \tag{2}$$

where $\mathbf{u}$ is a 3-dimensional velocity vector, κ is the vertical diffusivity, $F_{\mathrm{CO_2}}$ is the CO_2 flux, S_{bio} and S_{C} are the source/sink terms associated with biological activities and calcium carbonate flux, respectively. According to (2), the tendency of DIC is determined by advection, diapycnal mixing and addition/subtraction of DIC through biogeochemical processes and air-sea exchange whose rate is determined by the current $p\mathrm{CO_2}$ level through (1). When comparing the terms in ONLINE, CTRL and 5dAVG, excluding $F_{\mathrm{CO_2}}$, the biggest differences are found in $\kappa\partial^2\mathrm{DIC}/\partial z^2$ (Fig. 4(b); other terms not shown). Clearly the magnitude of the changes in diapycnal mixing term is sufficient to explain the CO_2 flux changes, indicating that the supply of carbon-rich water from below through vertical mixing is the primary driver.

The changes in CO_2 flux is the largest in the vicinity of the ACC. In summer when almost all regions in the model domain take up CO_2, suppressing processes with high temporal variability allows the ocean to absorb more CO_2 near the ACC (Fig. 5(a,c)). Although the changes in CO_2 flux north of the ACC and Brazil-Malvinas confluence zone are positive, they are not big enough to convert the CO_2 flux from the uptake to outgassing in CTRL. When NIWs are suppressed, the uptake of CO_2 becomes even stronger

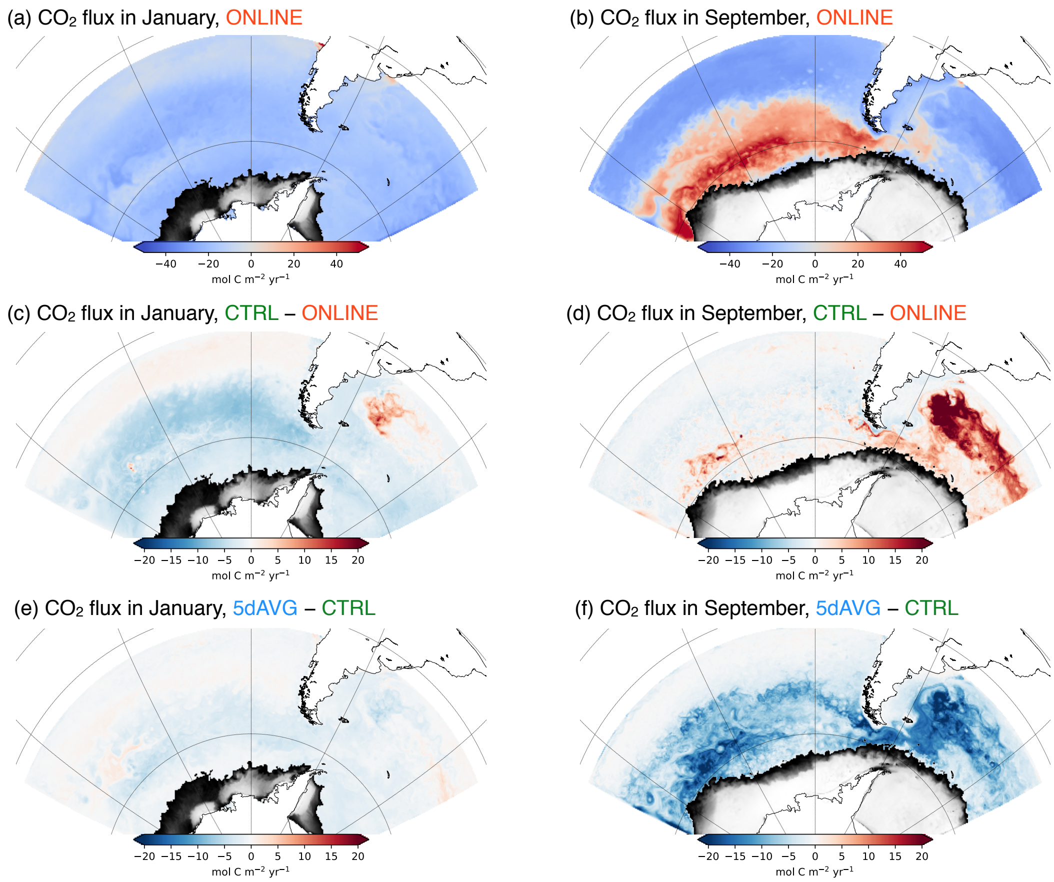

Figure 5. (a,b) Monthly averaged CO_2 flux in ONLINE, and (c,d) the difference between CTRL and ONLINE, and (e,f) between 5dAVG and CTRL. The panels on the left (a,c,e) are the CO_2 flux and its difference in January, and the panels on the right (b,d,f) are those in September. Similar to Figure 1, the gray mask near Antarctica represents the sea ice concentration.

mainly near the ACC in summer (Fig. 5(e)). In winter, using 5-day averaged physical fields and eddy diffusivity in the biogeochemical model does not alter the CO_2 flux as much as in summer near the ACC (Fig. 5(b,d)). The biggest changes are in the Brazil-Malvinas confluence zone. There is originally CO_2 uptake in ONLINE (Fig. 5(b)), but the positive difference between CTRL and ONLINE suggests CO_2 flux is close to zero or even positive (outgassing) in CTRL (Fig. 5(d)). The differences between 5dAVG and CTRL are negative (Fig. 5(f)), indicating that suppressing NIWs reduces CO_2 outgassing.

These spatial changes are closely linked to the changes in the vertical diffusive flux of carbon by diapycnal mixing. In summer, although the biological pump is the dominant term in (2) and leads to CO_2 uptake, the vertical diffusive flux tends to increased DIC at the surface (Fig. 6(a)). The difference in vertical diffusive flux of carbon between CTRL and ONLINE is generally negative, indicating the supply of carbon through vertical mixing is even weaker when high temporal variability is suppressed. 5dAVG shows even more reduction of carbon supply by vertical mixing when filtering out NIWs (Fig. 6(e)). The responses of the biological pump to suppressing high temporal variability and NIWs are not as large as those of vertical mixing (not shown), hence reduced supply of carbon from below leads to more uptake of CO_2 (Fig. 4(a) and 5(c,e)).

Changes in vertical diffusive flux of carbon can also explain the CO_2 flux changes between simulations in winter. In ONLINE, the carbon supply by diapycnal vertical mixing is the dominant signal at the upstream of the Drake Passage (Fig. 6(b)). When the biogeochemical model is driven by physical fields with the same mean states (including vertical mixing) but without high temporal variabilities (CTRL), the carbon supply to the surface by vertical mixing is enhanced in the upstream of the Drake Passage and Brazil-Malvinas confluence zone (Fig. 6(d)). However, when NIWs are suppressed (5dAVG), the vertical diffusive flux of carbon is reduced compared with CTRL (Fig. 6(f)) and even ONLINE (not shown). The reduction of carbon flux is particularly pronounced near the Drake Passage and vicinity of the ACC.

The results from ONLINE and 5dAVG demonstrate that suppressing NIWs and processes of high temporal variability shallows the MLD as shown in Figure 3. Since eddy diffusivity, κ, in the KPP scheme is proportional to the depth of surface boundary layer, it is the smallest in 5dAVG, leading to the weakest vertical diffusive flux of carbon to the surface. The decrease of carbon supply from subsurface lowers the $p\mathrm{CO}_2$ at the surface

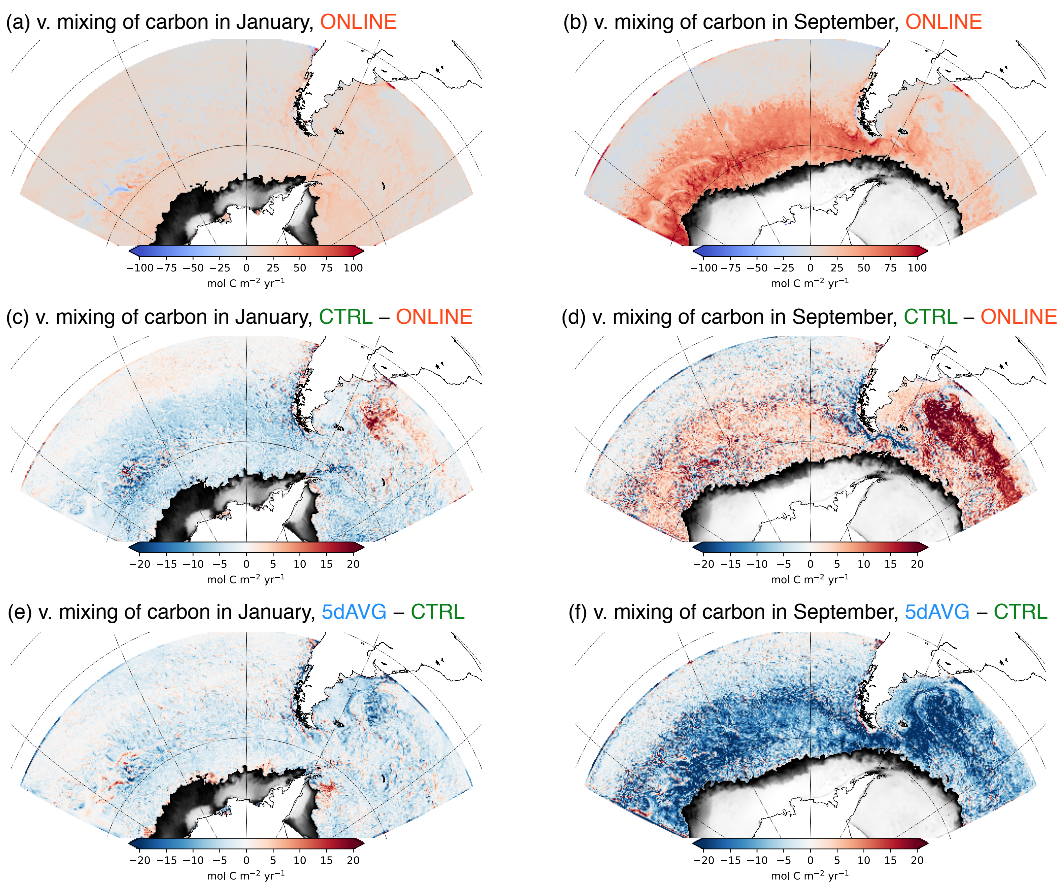

Figure 6. Same as Figure 5, but for the vertical mixing contribution to the surface DIC.

and causes more uptake of CO_2 in summer and less CO_2 outgassing in winter. Driving the biogeochemical model with the same mean states including vertical mixing but without processes of high temporal variability (CTRL) also modifies the diffusive flux of carbon, lowering surface pCO$_2$ in summer but increasing it in winter (Fig. 4(b), 6(c,d)). The effect of NIWs on CO_2 flux can be isolated by comparing CTRL and 5dAVG, and the comparison suggests that the effect of NIWs in CO_2 flux is greater in winter (Fig. 4(b), 6(e,f)). The decrease of carbon supply by vertical mixing can explain the reduced outgassing of CO_2 when NIWs are suppressed in winter (Fig. 5(f)).

4 Discussion

Three numerical experiments demonstrate the sensitivity of air-sea CO_2 flux to high-frequency processes. Weakening of vertical mixing leads to less supply of carbon-rich water from below and reduces the surface carbon concentration. Budget analysis of dissolved inorganic carbon (DIC) reveals that the diffusive carbon flux by vertical mixing is systematically lower when NIWs are suppressed (5dAVG; Fig. 4b). As a result, the SO emits less CO_2 in austral winter and takes up more CO_2 in austral summer, and this change is approximately 1/3 of seasonal variability in ONLINE.

We note that removing NIWs and processes with high temporal variability can potentially affect the air-sea CO_2 exchange by changing the solubility of the surface ocean. Temporal smoothing reduces the warm/cold temperature anomalies and increases/decreases solubility, resulting in the decrease/increase of partial pressure of CO_2 that changes CO_2 flux. However, we expect a very small net effect. The temporal smoothing preserves mean properties, hence there is no net sea surface temperature change. Since the changes in partial pressure of CO_2 with respect to temperature is fairly constant [*Takahashi et al.*, 1993], net-zero temperature change should yield a very small net change in partial pressure of CO_2.

We show that processes with a high temporal frequency such as NIWs have a significant impact on vertical mixing and CO_2 flux, suggesting that these processes must be resolved in numerical simulations for better estimation of CO_2 flux in the SO. In order to properly simulate NIWs, the frequency of the wind forcing should be higher than the local inertial frequency. The inertial frequency increases with latitude, and it is close to 2 cycles per day near $-75°$S, the southern boundary of our model (Fig. 2a). At this latitude, at least 6-hourly winds are required to accurately force NIWs. However, many models do not use wind forcing with the frequency adequate for resolving NIWs, including those in Coupled Model Intercomparison Project phase 5 (CMIP5): almost half of coupled climate models have daily coupling frequency [*Tian*, 2016]. Even eddy-resolving models may miss the energy associated with NIWs if the wind forcing frequency is lower than local inertial frequencies.

Our study demonstrates that NIWs have broad impacts not only on the surface ocean states but on the carbon cycle and air-sea CO_2 exchange through vertical mixing. The impact is the strongest near the ACC in winter where many climate models show a shallow MLD bias [*Downes et al.*, 2015]. The underestimation of the MLD can lead to not enough uptake of transient tracers (e.g., chlorofluorocarbons), and our study suggests that this could be in part due to the inability to fully resolve NIWs and associated mixing.

In recent years, the Southern Ocean Carbon and Climate Observations and Modeling (SOCCOM) project deployed floats with the ability to estimate the carbon concentration at the surface and CO_2 exchange between the atmosphere and the ocean. The new observations revealed that the wintertime CO_2 outgassing near the ACC had been underestimated by most numerical models. Hence it is important to evaluate whether NIWs are properly included in those numerical simulations in diagnosing the models' performance.

Acknowledgments

The MITgcm can be obtained from http://mitgcm.org. The surface forcing data used in this study are available at the Geophysical Fluid Dynamics Laboratory data portal webpage (http://data1.gfdl.noaa.gov/nomads/forms/core/COREv2.html). Resources supporting this work were provided by the NASA High-End Computing (HEC) Program through the NASA Advanced Supercomputing (NAS) Division at Ames Research Center with the award number SMD-15-5752. HS, JM, and DJM were supported by the NSF MOBY project (OCE-1048926 and OCE-1048897). HS acknowledges the support by Yonsei University Research Fund of 2018-22-0053. DJM also gratefully acknowledges NASA support.

References

Adcroft, A., C. Hill, and J. Marshall (1997), Representation of topography by shaved cells in a height coordinate ocean model, *Mon. Wea. Rev.*, *125*, 2293–2315.

Adcroft, A., C. Hill, J.-M. Campin, J. Marshall, and P. Heimbach (2004), Overview of the formulation and numerics of the MIT GCM, in *Proceedings of the ECMWF Seminar Series on Numerical Methods, Recent Developments in Numerical Methods for Atmosphere and Ocean Modelling*, pp. 139–149, ECMWF.

Alford, M. H., and M. C. Gregg (2001), Near-inertial mixing: Modulation of shear, strain and microstructure at low latitude, *J. Geophys. Res. Oceans*, *106*(C8), 16,947–16,968, doi:10.1029/2000JC000370.

Alford, M. H., J. A. MacKinnon, H. L. Simmons, and J. D. Nash (2016), Near-Inertial Internal Gravity Waves in the Ocean, *Annu. Rev. Mar. Sci.*, *8*(1), 95–123, doi: 10.1146/annurev-marine-010814-015746.

D'Asaro, E. (1985), The energy flux from the wind to near-inertial motions in the mixed layer, *J. Phys. Oceanogr.*, *15*, 1043–1059.

de Boyer Montégut, C., G. Madec, A. S. Fischer, A. Lazar, and D. Iudicone (2004), Mixed layer depth over the global ocean: An examination of profile data and a profile-based climatology, *J. Geophys. Res.*, *109*, C12,003, doi:10.1029/2004JC002378.

Dong, S., J. Sprintall, S. T. Gille, and L. Talley (2008), Southern Ocean mixed-layer depth from Argo float profiles, *J. Geophys. Res.*, *113*, C06,013.

Downes, S. M., R. Farneti, P. Uotila, S. M. Griffies, S. J. Marsland, D. Bailey, E. Behrens, M. Bentsen, D. Bi, A. Biastoch, C. Böning, A. Bozec, V. M. Canuto, E. Chassignet, G. Danabasoglu, S. Danilov, N. Diansky, H. Drange, P. G. Fogli, A. Gusev, A. Howard, M. Ilicak, T. Jung, M. Kelley, W. G. Large, A. Leboissetier, M. Long, J. Lu, S. Masina, A. Mishra, A. Navarra, A. J. George Nurser, L. Patara, B. L. Samuels, D. Sidorenko, P. Spence, H. Tsujino, Q. Wang, and S. G. Yeager (2015), An assessment of Southern Ocean water masses and sea ice during 1988–2007 in a suite of interannual CORE-II simulations, *Ocean Modell.*, *94*, 67–94, doi: https://doi.org/10.1016/j.ocemod.2015.07.022.

Dutkiewicz, S., A. Sokolov, J. Scott, and P. Stone (2005), A three-dimensional ocean-seaice-carbon cycle model and its coupling to a two-dimensional atmospheric model: uses in climate change studies, in *Joint Program on the Sci. Policy Global Change*, chap. Rep. 122, MIT, Cambridge, Mass.

Elipot, S., and R. Lumpkin (2008), Spectral description of oceanic near-surface variability, *Geophys. Res. Lett.*, *35*, L05,606, doi:10.1029/2007GL032874.

Follows, M. J., S. Dutkiewicz, and T. Ito (2006), On the solution of the carbonate system in ocean biogeochemistry models, *Ocean Modelling*, *12*, 290–301.

Holte, J., L. D. Talley, J. Gilson, and D. Roemmich (2017), An Argo mixed layer climatology and database, *Geophys. Res. Lett.*, *44*, 5618–5626, doi:10.1002/2017GL073426.

Jochum, M., B. P. Briegleb, G. Danabasoglu, W. G. Large, N. J. Norton, S. R. Jayne, M. H. Alford, and F. O. Bryan (2013), The impact of oceanic near-inertial waves on climate, *J. Climate*, *26*, 2833–2844.

Large, W., J. McWilliams, and S. Doney (1994), Oceanic vertical mixing: A review and a model with nonlocal boundary layer parameterization, *Rev. Geophys.*, *32*, 363–403.

Lenton, A., B. Tilbrook, R. M. Law, D. Bakker, S. C. Doney, N. Gruber, M. Ishii, M. Hoppema, N. S. Lovenduski, R. J. Matear, B. I. McNeil, N. Metzl, S. E. Mikaloff Fletcher, P. M. S. Monteiro, C. Rödenbeck, C. Sweeney, and T. Takahashi (2013), Sea-air CO_2 fluxes in the Southern Ocean for the period 1990-2009, *Biogeosciences*, *10*(6), 4037–4054, doi:10.5194/bg-10-4037-2013.

Marshall, J., C. Hill, L. Perelman, and A. Adcroft (1997a), Hydrostatic, quasi-hydrostatic, and nonhydrostatic ocean modeling, *J. Geophysical Res.*, *102*(C3), 5733–5752.

Marshall, J., A. Adcroft, C. Hill, L. Perelman, and C. Heisey (1997b), A finite-volume, incompressible Navier Stokes model for studies of the ocean on parallel computers, *J. Geophysical Res.*, *102*(C3), 5753–5766.

Marshall, J., H. Jones, and C. Hill (1998), Efficient ocean modeling using non-hydrostatic algorithms, *J. Mar. Syst.*, *18*, 115–134.

Parekh, P., M. J. Follows, S. Dutkiewicz, and T. Ito (2006), Physical and biological regulation of the soft tissue carbon pump, *Paleoceanography*, *21*, PA3001, doi: 10.1029/2005PA001258.

Sasaki, H., P. Klein, B. Qiu, and Y. Sasai (2014), Impact of oceanic-scale interactions on the seasonal modulation of ocean dynamics by the atmosphere, *Nature communications*, *5*, 5636.

Shao, A. E., S. Mecking, L. Thompson, and R. E. Sonnerup (2013), Mixed layer saturations of CFC-11, CFC-12, and SF_6 in a global isopycnal model, *J. Geophys. Res. Oceans*, *118*, 4978–4988, doi:10.1002/jgrc.20370.

Simmons, A., S. Uppala, D. Dee, and S. Kobayashi (2007), ERA-Interim: New ECMWF reanalysis products from 1989 onwards, in *ECMWF Newsletter*, vol. 110, pp. 25–35, ECMWF.

Simmons, H. L., and M. H. Alford (2012), Simulating the Long-Range Swell of Internal Waves Generated by Ocean Storms, *Oceanography*, *25*(2), 30–41, doi: http://dx.doi.org/10.5670/oceanog.2012.39.

Song, H., J. Marshall, P. Gaube, and D. J. M. Jr. (2015), Anomalous chlorofluorocarbon uptake by mesoscale eddies in the Drake Passage region, *J. Geophys. Res. Oceans*, *120*, 1065–1078, doi:10.1002/ 2014JC010292.

Song, H., J. Marshall, M. J. Follows, S. Dutkiewicz, and G. Forget (2016a), Source waters for the highly productive Patagonian shelf in the southwestern Atlantic, *J. Mar. Syst.*, *158*, 120–128.

Song, H., J. Marshall, D. R. Munro, S. Dutkiewicz, C. Sweeney, D. J. M. Jr., and U. Hausmann (2016b), Mesoscale modulation of air-sea CO_2 flux in Drake Passage, *J. Geophys. Res.*, *121*, 6635–6649, doi:10.1002/2016JC011714.

Tagliabue, A., J.-B. Sallée, A. R. Bowie, M. Lévy, S. Swart, and P. W. Boyd (2014), Surface-water iron supplies in the Southern Ocean sustained by deep winter mixing, *Nature Geoscience*, *7*, 314–320, doi:10.1038/ngeo2101.

Takahashi, T., J. Olafsson, J. G. Goddard, D. W. Chipman, and S. C. Sutherland (1993), Seasonal variation of CO_2 and nutrients in the high-latitude surface oceans: A comparative study, *Global Biogeochemical Cycles*, *7*(4), 843–878.

Takahashi, T., S. C. Sutherland, R. Wanninkhof, C. Sweeney, R. A. Feely, D. W. Chipman, B. Hales, G. Friederich, F. Chavez, C. Sabine, A. Watson, D. C. E. Bakker, U. Schuster, N. Metzl, H. Yoshikawa-Inoue, M. Ishii, T. Midorikawa, Y. Nojiri, A. Körtzinger, T. Steinhoff, M. Hoppema, J. Olafsson, T. S. Arnarson, B. Tilbrook, T. Johannessen, A. Olsen, R. Bellerby, C. S. Wong, B. Delille, N. R. Bates, and H. J. W. de Baar (2009), Climatological mean and decadal change in surface ocean pCO_2, and net sea-air CO_2 flux over the global oceans, *Deep-Sea Res. Pt. II*, *56*(8-10), 554–577.

Talley, L. D., G. Pickard, W. Emery, and J. Swift (2011), *Descriptive Physical Oceanography: An Introduction (Sixth Edition)*, 560 pp., Elsevier, Burlingham, MA.

Tian, F. (2016), Effects of coupling frequency on climate simulated by a coupled AO-GCM, Ph.D. thesis, Universität Hamburg Hamburg.

Tulloch, R., R. Ferrari, O. Jahn, A. Klocker, J. LaCasce, J. Ledwell, J. Marshall, M.-J. Messias, K. Speer, and A. Watson (2014), Direct estimates of lateral eddy diffusivity upstream of Drake Passage, *J. Phys. Oceanogr.*, *44*, 2593–2616.

Verdy, A., S. Dutkiewicz, M. J. Follows, J. Marshall, and A. Czaja (2007), Carbon dioxide and oxygen fluxes in the Southern Ocean: Mechanisms of interannual variability, *Global Biogeochem. Cycles*, *21*, GB2020, doi:10.1029/2006GB002916.

Wanninkhof, R. (1992), Relationship between wind speed and gas exchange over the ocean, *J. Geophys. Res.*, *97*(C5), 7373–7382, doi:10.1029/92JC00188.

Wetzel, P., A. Winguth, and E. Maier-Reimer (2005), Sea-to-air CO2 flux from 1948 to 2003: A model study, *Global Biogeochem. Cycles*, *19*, GB2005, doi: 10.1029/2004GB002339.